Influence of polymer morphology on the ability of imprinted network polymers to resolve enantiomers

Börje Sellergren* and Kenneth J. Shea*

Department of Chemistry, University of California, Irvine CA 92717 (USA)

ABSTRACT

Network copolymers imprinted with L-phenylalanine anilide (L-PheNHPh) exhibit an affinity for the print molecule. The binding of L-PheNHPh to the polymer can be quantitatively evaluated by employing the material as a stationary phase in a HPLC experiment. The degree of separation of the D and L enantiomers of PheNHPh (a value) is used to establish the influence of polymer morphology on polymer performance. Factors that promote stabilization of the template-polymer&able monomer complex prior to polymerization results in polymers with stronger and more selective binding of the substrate. Interestingly, a gel-like non-porous polymer performed similarly to a mesoporous polymer. Performance is also improved upon heat treatment of the polymers and various ways to inhibit the molecular recognition effect are demonstrated.

INTRODUCTION

During the last years, molecular imprinting or template polymerization has attracted considerable attention as a means of producing polymers exhibiting molecular recognition properties [1–21]. In this approach, a template is bound reversibly to functionalized monomers and co-polymerized in solution with a cross-linking monomer. The resulting polymer can be freed from template by hydrolysis or extraction. In a subsequent rebinding step the polymers bind with preference for the original template molecule in competition with structurally related molecules.

An approach based on the ability of the template and functional monomer to interact by non-covalent interactions with each other was employed in the imprinting of enantiomers of amino acid derivatives [7–9]. Highly cross-linked copolymers of **MAA** (methacrylic acid) and **EDMA** (ethyleneglycoldimethacrylate) proved to be the most efficient matrix in the molecular recognition process. In the liquid **chromato**graphic mode the polymers showed a pronounced selectivity for their original template molecule and in several cases base line separations of the corresponding enantiomers were achieved [10–12]. The polymers also were able to recognize subtle structural differences in the template. For instance enantiomer as well as substrate discrimination between phenylalanine anilide **(PheNHPh)** and phenylalanine N-methylanilide [13], carbobenzyloxyaspartic acid and carbobenzyloxyglutamic acid [12], and recently between phenylalanine ethyl ester **(PheOEt)** and diethyl-2-amino-3-phenylethylphosphonate **[Phe(P)(OEt)$_2$][14]** has been demonstrated.

For a systematic use of the template-imprinted polymers as chromatographic stationary phases it is of interest to understand the factors that affect the rebinding strength and selectivity as well as

* Corresponding author.
*Present address: Department of Analytical Chemistry, University of Lund, P.O. Box 124, S-22100 Lund, Sweden.

the factors underlying the extensive peak broadening that has so far been observed. The nature of the print molecule clearly affected these observations. For instance, print molecules containing two or three strong interaction sites (proton accepting or hydrogen bonding groups) towards methacrylic acid gave polymers exhibiting higher selectivity, stronger binding and broader peaks compared to polymers prepared using print molecules with fewer or weaker interaction sites (*cf.* L-PheNHPh *versus* L-*p*-amino-PheNHPh, L-PheOEt *versus* L-*p*-amino-PheOEt and L-PheOEt *versus* L-PheNHEt) [11]. It was therefore suggested that these results were due to the strength and molecularity of the association between the template and MAA prior to polymerization. This was supported by a H NMR and chromatographic study of a titration of the template L-PheNHPh with MAA [10]. The results showed that multimolecular assemblies between MAA and the print molecule existed in solution prior to polymerization. A complementarity between the functional groups at the binding sites and the template thus appears to play a major role in the molecular recognition process. Moreover the shape and rigidity of the template assemblies have been suggested to affect selectivity [10,12]. By carefully designed template imprinting systems based on reversible covalent interactions, the importance of the shape [15] and rigidity [16] of the template as well as the distance between the functional groups at the sites [17,18] have been assessed independently. Thus it was concluded that all factors affected the template rebinding selectivity.

Assuming the interactions between MAA and the print molecule to be electrostatic and hydrogen bonding in nature, the properties of the solvent (porogen) used in the imprinting step in terms of hydrogen bond capacity and polarity is likely to influence the strength of the interactions. Since these properties also are important in the solvation of the growing polymer chains and thus in the mechanism of pore structure formation, different porogens may lead to polymers with different morphologies. Likewise, other ways to promote the formation of template assemblies such as decreasing the polymerization temperature [20] or increasing the concentration of MAA in the monomer mixture [21] may also result in polymers with widely different morphologies.

Due to these complications an understanding of the individual role of the above-mentioned factors requires a study including a large number of polymers prepared under different conditions. Unambiguous relations between chromatographic performance (selectivity, retention and resolution) and polymer morphology on the one hand, and solubility parameters (hydrogen bonding, polar and dispersive) and polymerization temperature on the other is expected to give valuable information about the molecular recognition mechanism. In this study we have made a complete characterization of a number of imprinted polymers prepared in presence of L-PheNHPh as print molecule using various solvents as porogens. Moreover, thermally initiated and low-temperature photoinitiated polymers have been compared. The influence of functional and structural changes of the polymers were assessed by introducing variable length amide-based cross-linking monomers [22]. Finally, methods of inhibiting the specific rebinding were attempted as a way to gain insight into the molecular recognition mechanism.

EXPERIMENTAL

General procedures

D- and L-PheNHPh [10] and the bismethacrylamide monomers [22] were synthesized as described elsewhere. The methacrylate monomers were obtained from Aldrich. EDMA was purified by extraction with 10% sodium hydroxide brine and drying over anhydrous magnesium sulfate followed by distillation. MAA was purified by drying over anhydrous magnesium sulfate followed by distillation. The porogens were all distilled under a positive nitrogen atmosphere prior to use and all other reagents were purified according to standard procedures. The UV lamp used in the photopolymerizations was a medium-pressure mercury vapour lamp (Conrad-Hanovia) of 550 W with 33 W in the 320-400 nm interval. Scanning electron micrographs were obtained at the UCI Electron Microscope

Facility. The **FT-IR** spectrum was recorded on an Analect RFX 40 instrument, the differential scanning calorimetry (DSC) was performed on a DuPont 910 DSC instrument and **thermogravimetric** analysis (TGA) on a DuPont 951 TGA instrument. The **cross-polarization** magic angle spinning (CP-MAS) ^{13}C NMR spectra were kindly run by Prof. David Sherrington (University of Strathclyde, UK) on a Bruker **25-147MHz** instrument. All chromatographic evaluations were done using a Waters **484** UV detector, Waters 501 pump equipped with a **U6K** injector and a Hewlett-Packard integrating recorder.

Polymerizations

The polymers were prepared as shown in Scheme 1. To 3.8 ml (20 mmol) **EDMA,** 0.34 ml

(4 mmol) **MAA** and *240* mg (1 mol) **L-PheNHPh** in 5.6 ml porogen (resulting in Fm = volume porogen/total volume of porogen + monomers = 0.57) were added 40 mg (0.25 mmol) **azo-bis-** isobutyronitrile (AIBN) as initiator. The mixture was transferred to a **50-ml** thick-walled glass tube. This was freeze thaw degassed three times and sealed under vacuum. The thermally initiated polymerization was done at **60°C** in an oil bath (T-polymers) and the photochemically initiated polymerization (P-polymers) at 15°C in a thermostatted water bath (see also Table I for definition of polymer abbreviations). The tubes were symmetrically placed at *ca.* 10 cm distance from a UV light source and turned at regular intervals for a symmetric exposure. After 24 h the tubes were crushed and the polymers ground
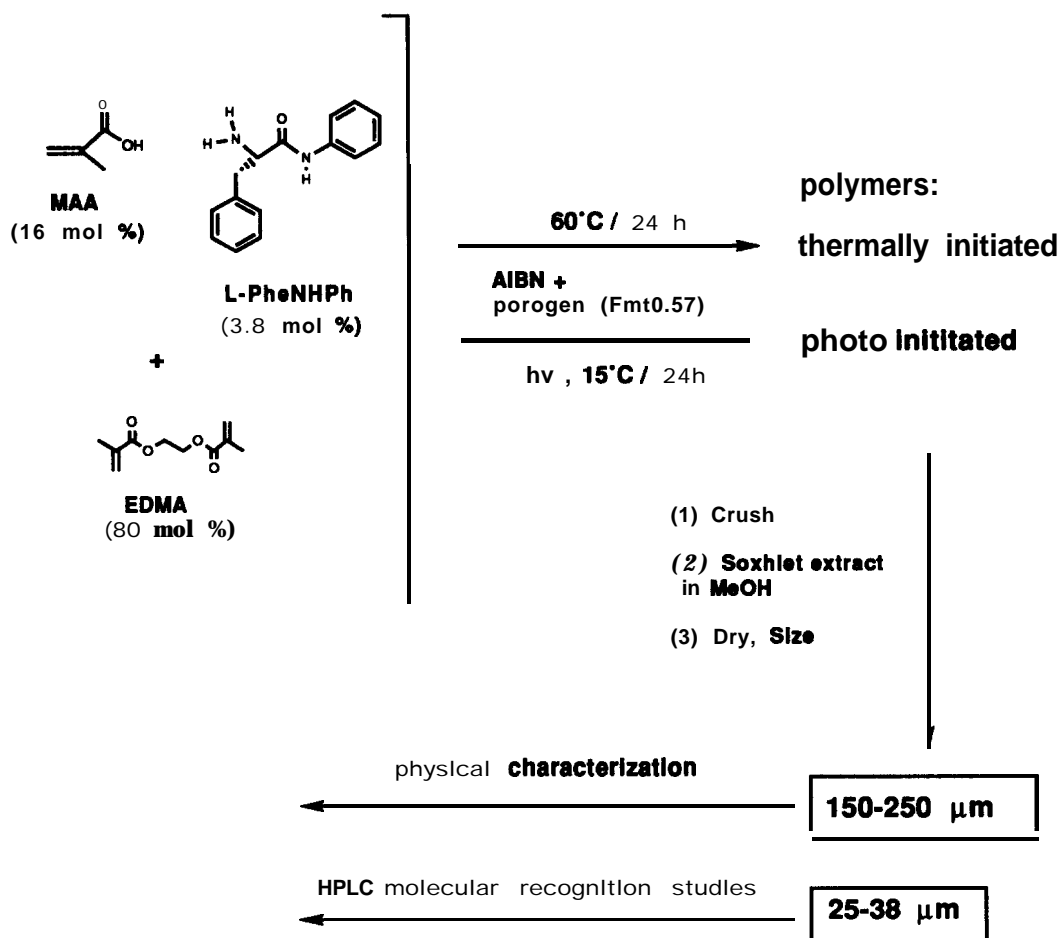
Scheme 1.

in a mortar, followed by soxhlet extraction in methanol for 12 h. The polymers were then dried overnight under vacuum at 50°C and sieved to a 150–250 μm and a 25-38 μm particle size fraction. The preparation of the polymers using the bismethacrylamide monomers is described in Table X. IR (KBr) of P1: 3458 (br), 2991, 2960, 1730, 1639, 1633, 1481, 1462, 1454, 1390, 1369, 1323, 1298, 1261, 1161, 1051, 957, 880, 816, 754 and 528 cm-'. CP-MAS ^{13}C NMR of P2 and T2: δ 177,168, 137, 127, 63 (br), 57 (br), 46, 24 (br), 19 ppm. The level of unsaturation was estimated by a comparison of the integrals at 177 and 168 ppm corresponding to non-conjugated and conjugated carbonylcarbons as described elsewhere [23].

Polymer density and solvent swelling studies

Dry polymer (1 ml, 150-250 pm) was placed in a 5-ml calibrated graduated cylinder and weighed. This gave the apparent dry density of the polymer. Excess solvent was then added and the polymer was stirred in order to remove air bubbles. The cylinder was then tapped until no further settling was observed. The swelling given as volume swollen polymer per volume dry polymer was read after 12 h. In another experiment swelling as a function of pH was studied. The polymer (0.5 ml, 150-250 pm) was placed in a volume-calibrated NMR tube and 2 ml MeCN–0.1 M NaCl (7:3) was added. Sodium hydroxide (1 M) was added in 40-μl increments with 3 h interval. Before each addition swelling and pH were measured.

Solvent uptake studies

Dry polymer (1.00 g, 150-250 pm) was placed in a scintillation vial and cyclohexane was added dropwise while the polymer was regularly agitated. Addition was stopped when the particles lost their ability to flow freely. The solvent was then allowed to evaporate until the particles just became free flowing. From the weight of the vial and the cyclohexane density, the solvent uptake, given as volume of solvent absorbed per weight of dry polymer, could be calculated.

Pore analysis

Pore and surface area analysis were performed by N_2 adsorption and Hg penetration on Micro-meritics ASAP 2000 and PS3200, respectively. In the N_2 adsorption a sample of polymer (150-250 pm) corresponding to *ca.* 20 m^2 (0.1-0.5 g) was degassed at 170°C overnight under vacuum. The adsorption and desorption isotherms were then recorded using a 200-point pressure table and 15 s equilibration time. This gave a pore size distribution of pores between 17 and 2000 A. In the Hg-penetration experiments a pore size distribution of pores between 1000 and 50000 Å was instead obtained. The surface area was determined using the BET model, the f-plot using Harkins-Jura average thickness equation and the pore distribution using the BJH model [24].

Splitting of template

The recovery of template after soxhlet extraction in methanol was determined by HPLC on a reversed-phase C $_{18}$ column using *p*-aminophenylacetate as internal standard and MeOH–3% HOAc (1:1) as eluent. All polymers except the one polymerized at 120°C [P1(120°C)] showed a recovery of 60–70%. Additional recovery is believed to occur upon acid wash since a high recovery (*ca.* 90%) has been observed by other techniques [8,10]. The polymer prepared at 120°C showed extensive breakdown of the template. The high accessibility of the carboxylic acid groups as indicated by the potentiometric titrations also indicates that the splitting yield is actually higher.

Chromatographic evaluation

The polymers with the 25-38 μm grain size fraction were slurry packed into 100-mm stainless steel columns [5 mm I.D. containing *ca.* 0.5 g (dry weight) of polymer after packing] using mobile phase A as solvent [MeCN–H_2O–HOAc (92.5:2.5:5, v/v/v)]. After having passed *ca.* 50 ml at a flow-rate of 10 ml/min the column was equilibrated at 1 ml/min until a stable base line was reached. The flow-rate was 1 ml/min, the volume of injected solute 10 μl and the detection wavelength 260 nm, unless otherwise stated. The capacity factor was calculated as $(t - t_0)/t_0$, where t is the retention time of the solute and t_0 the retention time of a non-retained void marker ($NaNO_3$). The separation factor (α) measures the relative retention between the enantiomers

$(a = k'_L/k'_D)$ and h the reduced plate height from the number of theoretical plates (n) as $h = L/(d_p n)$, where L = column length (10 cm), d_p = average particle diameter (31.5 μm) and n = $5.55(t/t_{1/2})^2$ ($t_{1/2}$ is the peak width at half height). The resolution factor R_s [W] and the asymmetry factor A, [26] were obtained graphically as described elsewhere.

Polymer esterification

Dry polymer, 0.52 g of **P1** and 0.41 g of **P1BL** of the **25–38-μm** grain size fraction, was agitated in 10 ml dry tetrahydrofuran (THF) in **50-ml** erlenmeyer flasks. Diazomethane, generated from 11.5 mmol of diazald (Aldrich), was added as an **etheral** solution giving a yellow color of the polymer slurry. The flasks were agitated gently and after addition they were closed with septa and opened to atmosphere with a small needle. After 12 h the color had faded and the addition was repeated. The yellow color now persisted and the excess diazomethane was quenched after

12 h with acetic acid. The polymers were then washed with excess THF and dried under vacuum at 50°C.

RESULTS AND DISCUSSION

Following the procedure shown in Scheme 1, a number of polymers were prepared by either photochemical or thermal initiation using L-PheNHPh as print molecule with solvents of various polarity and hydrogen bonding capacity as porogens (Table I). Polymers were also prepared excluding the print molecule (BL) or using benzylamine (BA) as print molecule. The polymers were then processed as indicated and subjected to physical characterization or to chromatographic evaluation.

Physical appearance, swelling and solvent uptake

Depending on which porogen was used either transparent, translucent or opaque polymers

TABLE I

SWELLING AND SOLVENT UPTAKE OF L-PheNHPh IMPRINTED POLYMERS

Polymer[a]	Porogen	Density[b] (g/ml)	Swelling[c] (ml/ml)	Solvent uptake[d] (ml/g)	Specific swelling[e] (ml/g)
T1	MeCN	0.35	1.19	1.12	3.4
T1BL	MeCN	0.31	1.19	1.11	3.8
T1BA	MeCN	0.38	1.31	1.10	3.4
T2	THF	0.38	1.27	1.11	3.3
P1	MeCN	0.38	1.36	1.00	3.6
P1BL	MeCN	0.34	1.31	1.07	3.9
P1BA	MeCN	0.36	1.31	1.12	3.6
P1(120°C)					
P2[f]	THF MeCN	0.36 0.52	1.84 1.35	0.53 1.03	3.8 3.5
P3[f]	CHCl$_3$	0.58	2.11	0.10	3.6
P4[f]	C$_6$H$_6$	0.40	1.55	0.91	3.9
P5[f]	DMF	0.51	1.97	0.38	3.9
P6[f]	CH$_2$Cl$_2$	0.58	2.01	0.14	3.5
P7	Isopropanol	0.29	1.10	1.14	3.8
P8	HOAc (glacial)	0.48	1.45	0.86	3.6

[a] The polymers were prepared as described in the experimental section and in Scheme 1 where T represents thermal initiation and polymerization at 60°C and P photochemical initiation and polymerization at 15°C. P1(120°C) was prepared by treating a polymer prepared as P1 at 120°C for 24 h before work up. BL indicates a blank polymer prepared in absence of template and BA a polymer prepared using benxylamine as template.
[b] Apparent density of 150–250-μm particles.
[c] Swelling in acetonitrile given as an average of two measurements with a spread of less than 3%.
[d] Volume of cyclohexane taken up per gram of polymer given as average of two measurements with a spread of less than 6%.
[e] Swelling divided by apparent density.
[f] These polymers appeared transparent.

were obtained. The transparent polymers cracked upon opening of the polymerization tubes and slowly turned opaque, probably due to shrinkage upon porogen evaporation. The shrinkage is reflected in the apparent dry density of the polymers (Table I). Indeed the polymers showing transparency had the highest density and thus shrunk the most upon drying. The gravimetric yields of polymerization was high (92-108%). It is interesting to note that the transparent polymers were prepared using porogens with a refractive index (n_D) (see Table V) higher than 1.4. Thus the transparency may be due to a refractive index match rather than to a certain pore structure.

In Table I swelling and solvent uptake data is seen for all the polymers in acetonitrile. Some general observations can be made. The photoinitiated polymers showed higher swelling than the thermally initiated ones. The same was true for the transparent polymers *versus* the opaque materials. If the swelling is expressed as the volume of swollen polymer per gram of dry polymer (specific swelling) it is seen that all polymers take up the same amount of acetonitrile indicating a fully reversible swelling-shrinking process as was seen in the polymerization of trimethylolpropanetrimethacrylate (TRIM) [27]. The uptake of cyclohexane is also given in Table I. Since little swelling was observed in this solvent the uptake data should reflect the permanent pore volume of these polymers. The photopolymers in general showed lower solvent uptakes than the corresponding thermally initiated polymers. The same relationship was observed for the transparent *versus* the opaque polymers. Interestingly a linear inverse relationship was found between the swelling and solvent uptake for these polymers, again indicating a reversible swelling-shrinking process. Polymer P6 was subjected to heat treatment in the dry state under vacuum. This resulted in a decrease in the swelling and solvent uptake in agreement with a recent study of TRIM polymers [27]. The decreased swelling was in the TRIM study explained by a heat-induced packing of the microspheres which could be reversed by heating the polymer in presence of solvent. The swelling was also studied in a series of solvents of different

TABLE II

SWELLING IN VARIOUS SOLVENTS

Swelling in ml/ml was determined in the various solvents as described in the experimental section. These values are averages of two measurements with a spread of less than 3%. The polymers were dried under vacuum at 60°C between measurements. MP = mobile phase used in the chromatographic evaluation: MeCN–H_2O–HOAc (96.25:1.25:2.5, v/v/v). L-10 represents addition of 10 mM of L-PheNHPh (template) to the swelling solvent.

Solvent	Polymers					
	T1	T1BL	T2	P1	P1BL	P 2
MeCN	1.19	1.19	1.31	1.36	1.31	1.84
MP	1.17	1.14	1.29	1.36	1.30	1.80
MeOH	1.17	1.19	1.30	1.37	1.29	1.83
Toluene	1.13	1.12	1.30	1.30	1.25	1.71
THF	1.19	1.17	1.30	1.35	1.31	1.79
H_2O	1.19	1.13	1.28	1.30	1.28	1.77
Cyclohexane	0.98	1.06	1.05	1.10	1.09	1.40
MeCN + L-10						1.87
MeCN + L-100						1.88
MeCN + D-10						1.93

ent polarity (Table II). The swelling was highest in the polar solvents (except for water) and lower in toluene and cyclohexane. According to the solubility parameters in Tables V and VI toluene and cyclohexane are poor solvents for linear co-polymers of MMA–EA–MAA (E A = ethylacrylate). No difference in swelling was observed when the experiment was performed in the presence of 10 or 100 mM template (L-PheNHPh) excluding any stabilizing cross-linking effect from the template. Swelling also tended to be lower for the blank polymers compared to the corresponding templated polymers (Table II). It is possible that the carboxylic acid dimers, which are more abundant in the blank polymer, serve as a non-covalent cross-linking agent.

Spectroscopic and thermal analysis

A typical FT-IR spectrum of a templated polymer is given in Fig. la. The resonances of interest from the vinyl and the carboxyl groups are indicated. The former may allow an estimate of the extent of unreacted double bonds and the latter give information of the hydrogen bonding state of the carboxyl groups. A well resolved
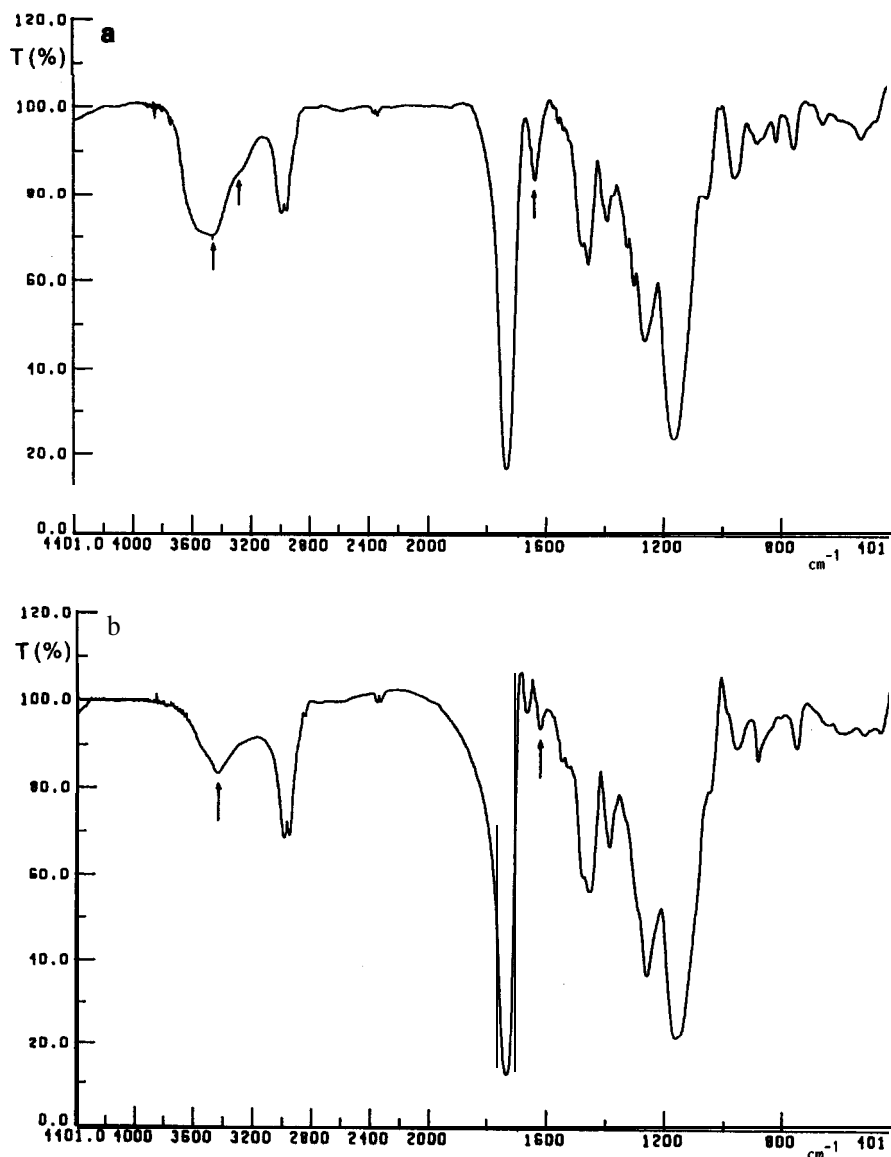
Fig. 1. FT-IR spectrum of (a) polymer P1(120°C) and (b) diazomethane-treated P1. The arrows at 3440 and 3300 cm^{-1} indicate the carboxylic acid OH stretch for the monomers and the hydrogen-bonded dimers, respectively and the arrow at 1639 cm^{-1} indicates the band arising from the vinyl-proton bonding.

band at 1639 cm-' is attributed to =C-H bending and the broad band at **3300–3700 cm^{-1}** to the carboxyl OH stretch. The **FT-IR** spectra of all polymers were indistinguishable indicating that they all contained approximately the same amount of unreacted double bonds and that no detectable difference in hydrogen bonding in the polymers is present. In IR studies on **MMA**–**MAA** copolymers [28] a band at 3300 cm^{-1} was attributed to carboxylic acid dimers while one at 3440 cm^{-1} was attributed to monomers. Interestingly a maximum was observed at 3440 cm^{-1} and an inflection at 3300 cm-'. However strong absorbance was also observed at a higher wavenumber indicating a population of isolated carboxylic acid groups.

Thermal analysis was performed by TGA and DSC. All of the polymers studied showed a high thermostability with no mass loss under 200°C. Between 220 and 480°C all mass was lost and in this interval the polymers showed variations in the onset of mass loss, the steepness of the mass loss curve and in the endotherms of decomposition (Table III). The thermally initiated polymers appeared slightly less stable than the photochemically initiated materials although they contain a lower amount of unreacted double bonds. Based on CP-MAS ^{13}C-NMR experiments on T2 and P2 a level of unsaturation of cu. 6 and 9%, respectively, was found. Moreover, polymer P6, which belongs to the gel-like non-porous materials, showed a higher stability than P1 which is mesoporous. These variations may be related to the polymer morphology.

Pore analysis

Nitrogen adsorption-desorption and mercury porosimetry are techniques for the determination of polymer pore structures in the dry state [24]. Nitrogen sorption commonly revealed Type IV isotherms which indicate mesoporosity (Fig. 2a). Most of the polymers showed a hysteresis loop where the desorption branch did not close but leveled off either below or above the adsorption branch. This was pronounced for the polymers

TABLE III

THERMOSTABILITY OF IMPRINTED POLYMERS

The temperatures for 0 and 100% mass loss were determined from the point where the trace departed from or reached the base line.

Polymer	Temperature (°C) at x% mass loss				
	0	25	50	75	100
T1	235	340	375	415	468
T1BA	250	369	399	420	460
T2	246	315	357	405	458
P1	229	377	404	430	465
P1BL	225	372	409	436	485
P1BA	240	363	395	421	465
P2(120°C)	232	363	397	423	460
P6	234	392	419	435	474

exhibiting the highest swelling and the lowest solvent uptake (Table I). Such behavior has been explained by shrinking of the polymer when subjected to increasing pressure at the liquid N_2 temperature and thus entrapment of N_2 molecules inside the polymer matrix [29]. During gas release from the pores of a certain size a lower relative pressure is thus required than one that can be calculated from the Kelvin equation [24]. Possibly the shrinking effect can be reduced by using a gas with lower saturation pressure P_0 (CO,) which would allow measurements at a higher temperature [29]. It should be noted that some of the polymers, in particular those which previously showed the lowest solvent uptake and the highest swelling (Table I), strongly retained the helium used in the free volume measurements. As a result, manual degassing had to be applied at elevated temperatures (170°C) after the cold free space measurement.

Since the adsorption average pore diameter was in closer agreement than the desorption diameter with values obtained from the BET calculation the former is reported in Table IV In general a narrow size distribution in the desorption plot (Fig. 2b) and a lower average pore diameter compared to the adsorption plot (Fig. 2c) indicates the existence of "bottle shape" pores [24]. The results of the study is summarized in Table IV The polymers showed a wide distribution of surface areas and pore volumes. P3 and P6 were non-porous with essentially no surface area or internal pore volume. P7 on the other hand showed a macroporous character requiring Hg porosimetry (>1000 A) to include all pores. The remaining polymers were mesoporous in character.

Particle texture

Scanning electron micrographs reveal the difference in morphology between the polymers (Fig. 3). Polymer P6, which belongs to the non-porous materials, shows a smooth featureless image with no observable pores. Fractures were observed probably arising from stress created during shrinking. P7 on the other hand showed a rough surface with clearly visible pores. A trend towards rougher surfaces and larger pores was
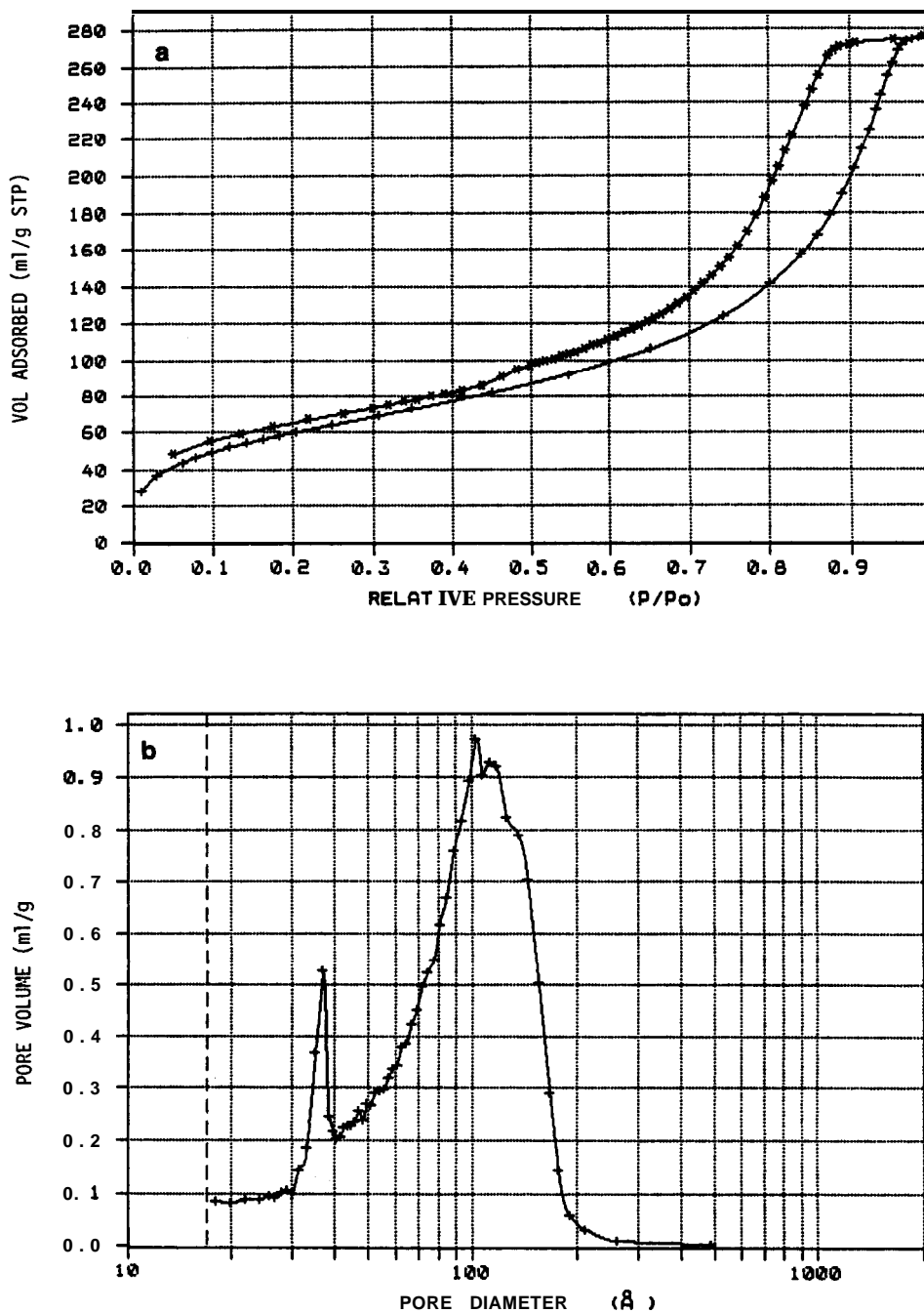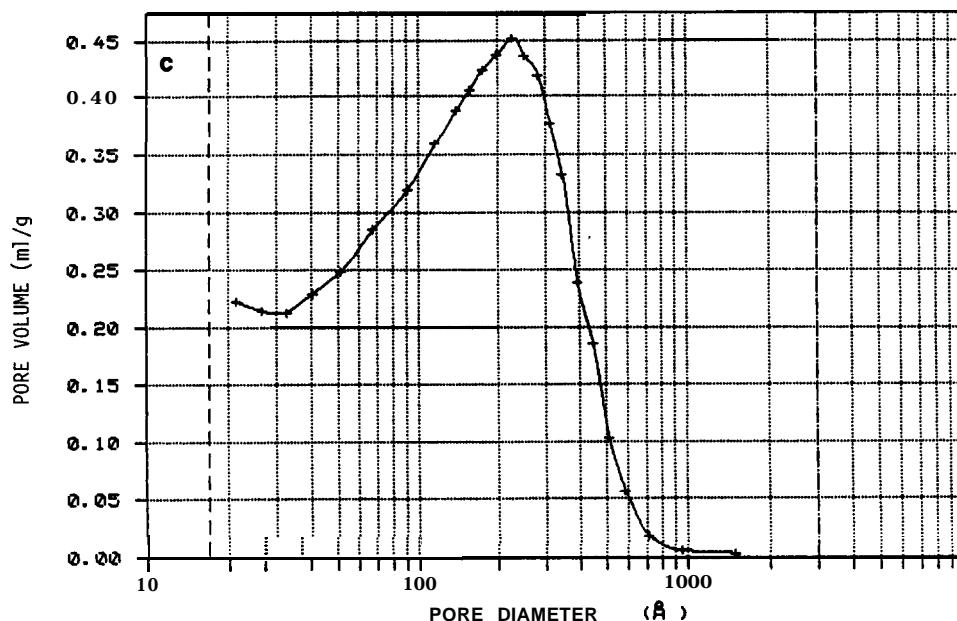
Fig. 2.

Fig. 2. (a) Nitrogen adsorption-desorption isotherm of polymer **P1** after helium outgassing at 150°C. + = adsorption; * = desorption. (b) Pore size distribution calculated using the BJH model on the desorption isotherm. (c) As in b on the adsorption isotherm. P_0 = nitrogen saturation pressure, STP = standard temperature and pressure.

seen in the order: P6 < P1 < T1 < P7 which is in agreement with the pore analysis (Table IV).

Aspects of polymer pore structure formation

In the imprinting process low-temperature polymerization is preferable for several reasons. When the template interacts by non-covalent interactions with the monomers a negative AS for complex formation will favor complexation at low temperature. Side reactions may be minimized in particular for labile templates. Lower temperatures will lower the number of stable conformers which in turn may lead to sites of a more defined geometry. In spite of these advantages free radical polymerization of network polymers at low temperature can result in undesired changes in polymer morphology. Often a large portion of unreacted double bonds remains in the polymer leading to high swelling, low pore volume and low surface areas [27]. These changes may adversely affect the rebinding selectivity. In this study a complete polymer characterization is therefore necessary.

Knowledge about the solubility parameters (δ) for the porogen and the polymer allow an estimate of the heat of mixing per unit volume according to:

$$\Delta H_{\mathrm{m}}/V = (6, -\delta_2)^2 \Phi_1 \Phi_2 \tag{1}$$

where δ_1 is related to the energy of vaporization of species 1 and Φ_1 its volume fraction in the mixture (species 1 and 2 are assumed to be non-interacting) [30]. A minimum AG is obtained when $\delta_1 = \delta_2$ implying a maximum solvation of the growing polymer chains (good solvent). In Table V the porogens have been classified according to their solubility parameter divided into a dispersive, a dipole-dipole and a hydrogen bond term [30]. Depending on the size of the hydrogen bond term the porogens have been further classified as either poorly, moderately or strongly hydrogen bonding. A correct estimate of δ of the polymers is difficult due to their cross-linked nature which gives rather small swelling factors. Often however the solubility parameter is close to the one of the predominat-

TABLE IV

SURFACE AREA AND PORE ANALYSIS ON THE IMPRINTED POLYMERS

Polymer	N$_2$ adsorption					Hg porosimetry		
	Surf. area (BET) (m^2/g)	Pore volume* (ml/g)	Pore diameter' (A)	Micropore volume^d (ml/g)	Micropore surf. area^d (m^2/g)	Pore volume' (ml/g)	Surf. area' (m^2/g)	Pore diameter' (A)
T1	317	0.89	118	0.036	85	0.04	1	1500
T1BL	326	0.89	119	0.051	109			
T1BA	276	0.82	123	0.030	67			
T2	382	0.73	89	0.054	116			
P1	256	0.60	94	0.012	30	0.06	1.5	1500
P1BL	267	0.72	91	0.009	31			
P1BA	253	0.66	104	0.011	34			
P1(120°C)	266	0.65	%	0.010	33			
P2	194	0.24	52	0.006	16			
P3	3.5	0.007	91	0.0004	0.9			
P4	216	0.43	78	0.005	15			
P5	127	0.17	52	0.002	9.7			
P6	3.8	0.007	71	0.0003	0.9	0.02	02	1500
P7	49	0.20	121	0.003	9.0	0.74	11	1800
P8	267	0.52	77	0.008	29			

^{a} Determined using the BET model on a seven-point linear plot.
^{b} BJH cumulative adsorption pore volume of pores between 17 and 3000 A.
^{c} BJH adsorption average pore diameter (4·pore volume/surface area) of pores between 17 and 3000 A.
^{d} Based on a r-plot using Harkins-Jura average thickness.
^{e} Cumulative pore volume and surface area of pores between 1000 Å and 10 μm.
^{f} Average pore diameter of pores between 1000 Å and 10 μm calculated as 4·pore volume/surface. area.

ing monomer. As seen in Table VI all porogens have δ values in the range of either *p*-MAA, p-MMA or p-MMA-MAA-EA.

The mechanism of pore structure formation in network polymers has been thoroughly reviewed [31,32]. A detailed analysis of polymer pore structure formation in the preparation of highly cross-linked TRIM was recently reported [27]. It is particularly interesting to note the influence of the solvating ability of the porogen on the pore structure formation. Performing the polymerization in a good solvent (toluene) favors inter-molecular cross-links giving a relatively homogeneous network. The phase separation is controlled by the formation of solvent swollen gel particles which coagulate to form grains. These in turn coagulate to build up the pore system of the polymer. The links between the grains appear to be flexible since this type of polymer shrinks upon drying and swells to the original volume upon reimmersion in solvent. A poor

solvent (isooctane) will promote agglomeration leading to the formation of dense highly cross-linked microspheres. The phase separation under these conditions is controlled by precipitation of the microspheres giving a relatively open pore structure where the strong links between the microspheres produce less shrinking and swelling. It should be noted that the number of residual double bonds in the polymers was about the same. Therefore, the authors did not attribute the different swellings to variable levels of cross-linking.

As seen in Table IV and from the structural data (Table I) no obvious correlation exists between $(\delta_1 - \delta_2)^2$ (Tables V, VI) and the polymer morphology in the present study. However in analogy with the TRIM system [27], the specific swelling (volume of polymer plus acetonitrile per gram of dry polymer) of the polymers was constant regardless of the dry state morphology and volume swelling. In addition, the
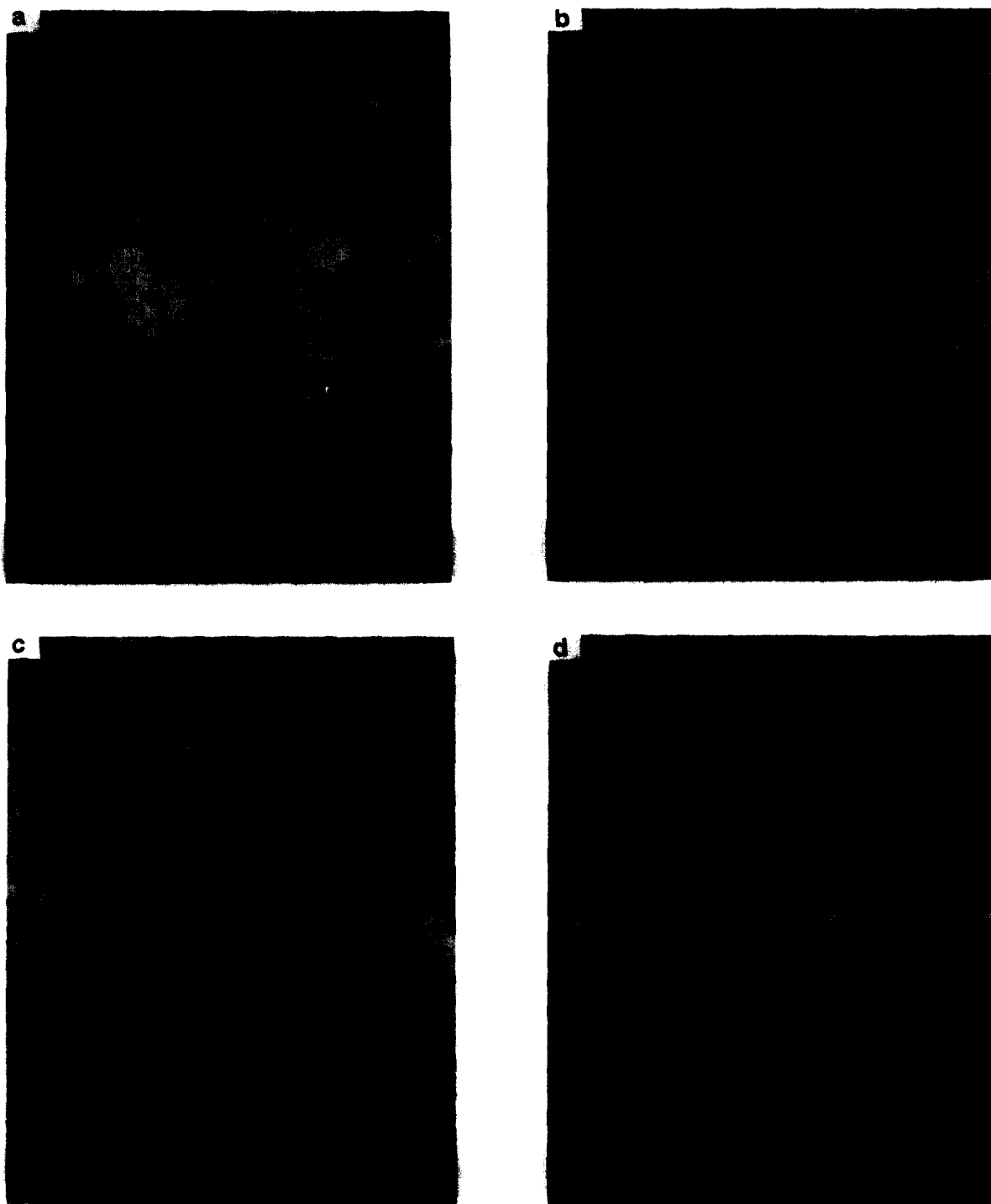
Fig. 3. *Scanning* electron micrographs of (a) P6, (b) P1, (c) T1 and (d) P7 photographed at 8000× magnification.

TABLE V

SOLUBILITY PARAMETERS, HYDROGEN BOND CAPACITY AND REFRACTIVE INDICES OF THE SOLVENTS [30]

The solubility parameter δ has been divided into a dispersive term δ_d, a polar term δ_p and a hydrogen bond term δ_h. H bond is a measure of the hydrogen bond capacity of the solvent in terms of both donor and acceptor ability, P = poor, M = moderate and S = strong. n_D = Refractive index.

Solvent	δ_d	δ_p	δ_h	δ (MPa$^{0.5}$)	H bond	n_D
MeCN	15.3	18.0	6.1	24.6	P	1.34
THF	16.8	5.7	8.0	19.4	M	1.41
CHCl$_3$	17.8	3.1	5.7	19.0	P	1.45
C$_6$H$_6$	18.4	0	2.0	18.6	P	1.50
DMF	17.4	13.7	11.3	24.8	M	1.43
CH$_2$Cl$_2$	18.2	6.3	6.1	20.3	P	1.42
Lsopropanol	15.8	6.1	16.4	23.5	S	1.38
HOAc	14.5	8.0	13.5	21.3	S	1.37
MeOH	15.1	12.3	29.3	29.7	S	
Toluene	18.0	1.4	2.0	18.6	P	
H$_2$O	15.5	16.0	42.4	47.9	S	
Cyclohexane	16.8	0	0.2	16.8	P	

TABLE VI

SOLUBILITY PARAMETERS OF POLYMERS IN SOLVENTS OF DIFFERENT HYDROGEN BOND CAPACITY [30]

The solubility parameter ranges were obtained for commercial polymers given in the Polymer Handbook [30].

Polymer	δ (MPa$^{0.5}$) Solvent hydrogen bonding capacity		
	Poor	Moderate	Strong
MMA	18.2-26	17.4-27.2	0
MAA	0	20.3	26.0–29.7
MMA–EA–MAA (40:40:20 mol%)	0	18.2-22.1	19.4-29.7

number of residual double bonds appeared to be about the same for all polymers (see under spectroscopic analysis). It is therefore possible that a similar mechanism as proposed for the TRIM polymerization is operating in the template polymerizations in this study. This implies that the swollen state morphology of the polymers may be quite similar.

Polymer selectivity

All the polymers were initially evaluated in the liquid chromatographic mode for their ability to separate D- and L-PheNHPh using the standard criteria for chromatographic characterization [26]. These include the polymer selectivity reflected in the separation factor (a), the binding reflected in the retention or the capacity factor (*k'*), the column efficiency or dispersion reflected in the reduced plate height (*h*), band spreading due to slow adsorption-desorption kinetics or a non-linear binding isotherm reflected in the peak asymmetry (*A,*) and finally the efficiency of a separation reflected in the resolution (*R$_s$*). Due to peak asymmetry (mainly for the mostly retained enantiomer) the assumptions that the peak retention time is equal to the peak maximum retention time and that the peak width is proportional to the peak standard deviation are now only approximations. However since the L peak exhibits tailing the true retention time should be longer. The given α values are therefore low estimates of the true values. The eluting strength of the mobile phase was chosen in order to balance the interactions between the solute and the stationary phase. In this regard the existence of mobile phase complexes has earlier been shown and in addition a quantitative analysis of their stability has been presented [10]. The mobile phases were: A= 92.5:2.5:5 and B = 96.25:1.25:2.5 (v/v/v) MeCN–H$_2$O–HOAc. This gave in all cases a *k'* of the least retained

solute between one and two allowing a more accurate determination of the separation factor α, i.e. a determination that is less dependent on an accurate determination of the void elution. The latter was determined using acetone as void marker which in the mobile phase coeluted with acetonitrile and sodium nitrate.

In Table VII the α values obtained at two sample loads for all polymers are shown. In addition results from the swelling and pore analysis as well as the hydrogen bonding capacity of the porogen has been included. As mentioned above, the polymer morphology in the dry state range from gel-like non-porous with a high swellability (P3, **P6**) to macroporous with a lower swellability **(P7)**. Since the mass-specific swelling is similar for all polymers (Table I) the polymers may show a more similar morphology in the swollen state. *Nevertheless, no obvious correlation appears to exist between selectivity and polymer morphology. Instead, a correlation between the hydrogen bonding capacity of the porogen and the polymer selectivity can be seen.*

Thus a trend towards lower α values upon increase in the hydrogen bonding capacity of the porogen is observed. This is in line with the previously proposed recognition model based on ion-pairing and hydrogen-bonding interactions [10]. A similar trend is seen for the thermally initiated polymers which as expected showed lower selectivity than the photoinitiated polymers. It should be noted that neither the dipole nor the dispersion term show any correlation with the polymer selectivity (*cf.* Tables **V**, VII).

Polymer saturation capacity

Using the mobile phase A unusual **chromato-**graphic behavior was seen in the low concentration regime (<100 nmole applied), leading to peak splitting and local minima and maxima in the plots of k' and α *versus* sample load. The origin of these effects are mainly mobile phase related and probably involve slow mobile phase equilibria with acetic acid [14]. By using buffered mobile phases these problems were eliminated. By increasing the sample load of D,L-**PheNHPh**

TABLE VII

CHROMATOGRAPHIC ENANTIOMER SELECTIVITY AND RESULTS FROM THE SWELLING AND PORE ANALYSIS IN RELATION TO HYDROGEN BOND CAPACITY OF POROGEN

The chromatographic separations were carried out as described in the experimental section using a mobile phase: MeCN–H_2O–HOAc, 92.5:2.5:5 %, v/v and applying two different sample loads of D,L-PheNHPh. NR = non-resolved peak maxima.

Polymer	Porogen	H bond type	Swelling (ml/ml)	Pore volume (ml/g)	Surface area (m^2/g)	Separation factor α ($= k'_L/k'_D$) Sample load of D,L-**PheNHPh**	
						12.5 nmol	loo nmol
P1	MeCN	P	1.36	0.60	256	5.8	2.6
P3	CHCl$_3$	P	2.11	0.007	3.5	4.5	2.6
P4	C$_6$H$_6$	P	1.55	0.43	216	6.8	2.4
P6	CH$_2$Cl$_2$	P	2.01	0.007	3.8	8.2	2.4
P5[a]	DMF	M	1.97	0.17	127	2.0	NR
P2	THF	M	1.84	0.24	194	4.1	1.5
P7[a]	Isopropanol	S	1.10	0.86	49	3.5	2.4
P8[a]	HOAc	S	1.45	0.52	267	1.9	NR
T1	MeCN	P	1.19	0.89	317	3.1	NR
T2	THF	M	1.27	0.73	382	1.6	NR
P1(120°C)	MeCN	P	1.35	0.65	266	3.7	2.4
P6(120°C)[b]	CH$_2$Cl$_2$	P	1.90	–	–	NR	2.3

[a] Mobile phase MeCN–H_2O–HOAc, 96.3:1.2:2.5 %, v/v.
[b] Treated under vacuum in the dry state at 120°C for 24 h. Solvent uptake: 0.09 ml/g.

the separation factor typically decreased rapidly, leveling off at a sample load of *ca.* 100 nmol (Fig. 4a). The steepness of the slope depended on porogen, polymerization temperature as well as on eventual heat treatment of the polymer. This is in qualitative agreement with our earlier published binding study on thermally initiated polymers at elevated column temperature although a higher saturation capacity was in that case observed [11]. By finishing the polymerization for 24 h at 120°C [P1(120°C)] a polymer that showed higher saturation capacity and improved chromatographic performance was obtained

(Fig. **4**), reflected in the higher resolution factors (R_s) observed for this polymer. *It is clear from earlier reported saturation capacities of imprinted polymers that polymers prepared by thermal initiation [10] are superior to those prepared by photoinitiation [20] allowing in the former case sample loads of ca. 2.4 mg/g (column temperature: WC) and in the latter case 0.5 mg/g polymer, respectively with resolved peak maxima.* It should be noted that the saturation capacity (number of available binding sites) of the polymers in this study is low in relation to the amount of template added to the monomer
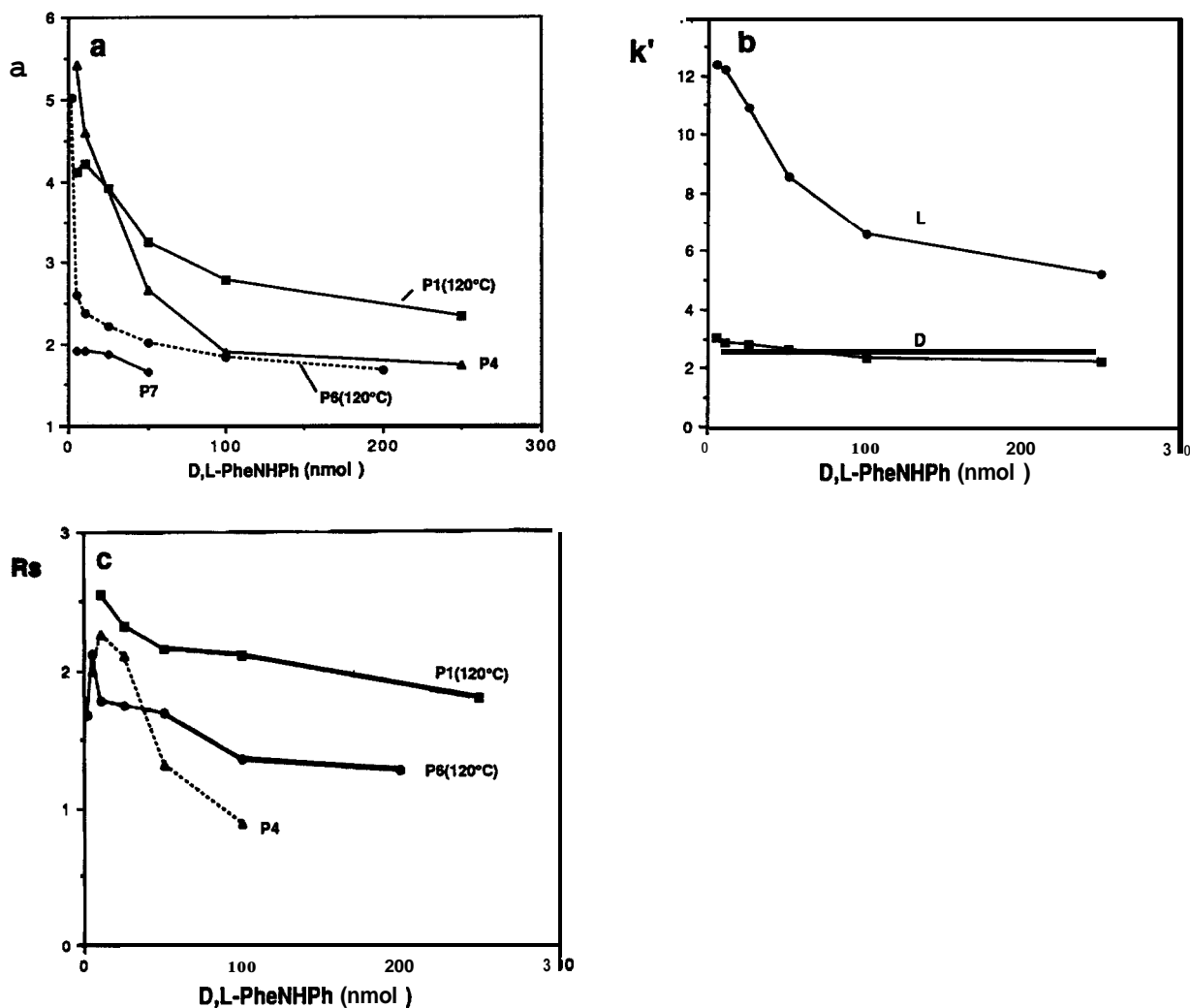

Fig. 4. (a) Separation factor (a), (b) capacity factor (k') of P1(120°C) and (c) resolution (R_s) *versus* sample load on various polymers in the study using MeCN–0.05 M potassium phosphate (KP) buffer pH 7 (7:3) as mobile phase.

mixture (theoretical maximum number of sites). This number can be estimated from the loading factor giving column overloading [34]. Severe overloading normally occurs at loading factors well below the saturation capacity of the column (5–10%). This corresponds to a saturation capacity of cu. 20 μmol/g for polymer P1(120°C) which implies that only 10% of the theoretical maximum number of sites are active. Similar low saturation capacities were observed in independent batch and frontal chromatographic binding studies [21,35]. In these studies a **monosite Langmuir** isotherm was assumed. In view of the site heterogeneity as indicated by Fig. 4 a **Langmuir** binary site model as proposed by Dickey [36] several years ago may better describe the observed binding isotherm. Alternatively a multisite model as described by Wulff et *al.* [37] may be used where an association constant for each newly covered site is calculated.

In studies employing reversible covalent binding between the functional monomer and the print molecule clearly higher saturation capacities are observed allowing a 2-3 fold excess of substrate to sites to be applied in the rebinding studies [15–19]. This typically results in cu. 90% rebinding based on the splitting yield. In non-covalent imprinting higher saturation capacities

can be expected by using lower polymerization temperatures, a larger amount of functional monomer or by matching functional groups that are known to interact strongly in solution.

Effect of heat treatment on chromatographic performance

In view of the previously reported swelling effects upon heat treatment of TRIM polymers [27], the effect of such treatment upon the chromatographic performance was investigated. Two photoinitiated polymers showing different dry state morphologies were subjected to heat treatment in the dry state (Table VIII). For the gel-like polymer (P6) this resulted in a lower swelling (see Table VII) and lower α values at low sample loads (mobile phase A). The decrease in selectivity appeared to be reversible since, after a prolonged run in buffered mobile phases, a repeated run using mobile phase A resulted in high α values at low sample loads. In the buffered mobile phase at pH 7 the polymer exhibited high efficiency with low h and high R_s comparable to P1(120°C) (Fig. 5). At pH 7 the polymer was then subjected to additional heat treatment. This had only little effect on the selectivity and performance.

These results contrasted with results obtained

TABLE VIII

EFFECT OF HEAT TREATMENT ON CHROMATOGRAPHIC PERFORMANCE OF POLYMER P4 AND P6

The chromatographic experiments were performed using as mobile phase **MeCN–0.05 M** KP buffer, **pH** 7 (7:3) at a flow-rate of 1 **ml/min** and injecting 10 nmol of D,L-PheNHPh as described in the experimental section. NR = no enantiomeric resolution. **VB** = very broad.

Treatment	Stationary phase	k'_L	a	h_D	h_L	h_0	R_s
None	P4	8.3	4.1	32	138	7	2.2
	P6[c]	6.9	8.2	77	264	26	1.5
Heat 120°C, 17 h dry[a]	P4	4.6	2.1	30	99	8	1.5[d]
	P6[c]	0.8	NR	113		6	NR
	P6	4.4	2.0	23	35	6	1.9
Heat 130°C, 4 h in mobile phase[b]	P4	1.9	1.6	158		14	<1[d]
	P6[c]	16	6.4	106	VB	8	1.8
	P6	5.7	2.3	33	91	10	1.7

[a] The polymer was heated under vacuum **followed** by column repacking.
[b] The column was immersed in an **oil** bath and heated keeping the flow-rate at 1 **ml/min**.
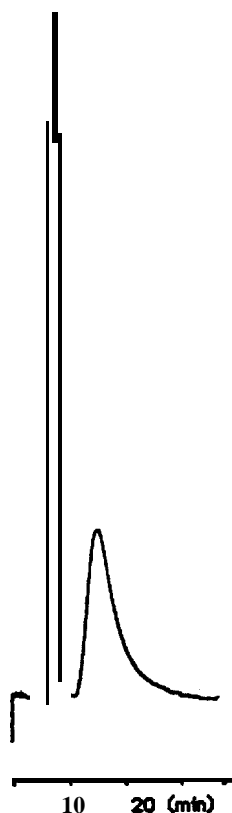[c] Mobile phase: **MeCN–HOAc–H$_2$O** (92.5:5:2.5, v/v/v).
[d] Column length: 5 cm.

Fig. 5. Elution profile of 10 nmol D,L-PheNHPh applied on an L selective heat treated polymer (P6) using as mobile phase: MeCN–0.05 M KP buffer, pH 7 (7:3) at a flow-rate of 1 ml/min.

using the more porous polymer (P4). After initial dry heat treatment lower k' and α were observed as well as a poorer, performance (higher h). This trend continued upon the subsequent wet heat treatment. The seemingly higher thermostability of the gel-like polymer (P6) was also indicated by the thermal analysis (see Table III). Variable temperature runs on this polymer may therefore allow an estimate of the **energetics** of the binding.

Chemical modifications affecting binding and selectivity

The photoinitiated template and plank polymers prepared using acetonitrile as porogen (**P1** and **P1BL**) were treated with a large excess of diazomethane for **48** h. This was followed by a reinvestigation of swelling, solvent uptake, FT-IR, DSC, TGA and chromatographic performance (Table IX). A somewhat lower swelling and solvent uptake was observed. Interestingly a clear loss of selectivity is seen in the large decrease in the separation factor showing the importance of the ion pair and hydrogen bonding interactions for recognition. In the IR spectrum (Fig. lb) only part of the OH band disappeared, mostly the **absorbances** at higher wavenumbers. This is to be expected since the free carboxylic acid groups should be more reactive than the hydrogen bonded groups. Also a large decrease in the vinyl band at 1639 cm-' was seen probably due to a **1,3** addition of diaxomethane to unreacted double bonds. Thus a large proportion of unreacted double bonds seems to be accessible. The DSC and TGA traces for both polymers were almost identical. An endotherm at low temperature was observed corresponding to a mass loss which could be attributed to the weight of a methylester group. This was not observed in

TABLE IX

INHIBITION OF SUBSTRATE RECOGNITION

The diazomethane and base treatment was performed on polymer P1 and P4, respectively, as described in the Experimental section. The mobile phase was MeCN–H_2O–HOAc (92.5:2.5:5 %, v/v) and the sample load was 10 nmol of D,L-PheNHPh.

Treatment	State	Swelling (ml/ml)	Solvent uptake (ml/g)	k'_L	a ($= k'_L/k'_D$)
CH_2N_2	–COOH	1.36	0.78	7.5	5.8
	–COOMe	1.28	0.68	1.7	1.4
MeOH–10% NaOH	Unhydrolyzed	1.55		2.0	5.6
(4:1%, v/v)	Hydrolyzed	1.70		1.2	2.3

the untreated polymer. In another experiment the polymers were stirred at room temperature in **MeOH–10% NaOH (4:1)** overnight. This gave rise to a substantial release of methacrylic acid and a higher swelling. The treatment resulted in a partial loss of selectivity and binding (Table IX). The increase in swelling has been attributed to hydrolysis of cross-links in the polymer [33] which may explain the partial loss of selectivity due to the larger degree of flexibility in the polymer backbone.

Use of bismethacrylamides in non-covalent imprinting

The use of bismethacrylamides as functional monomers in non-covalent imprinting was evaluated by preparing a series of polymers as indicated in Table X. The chromatographic

TABLE X

EVALUATION OF BISAMIDE CROSS-LINKERS IN THE IMPRINTING OF L-PHENYLALANINE ANILIDE

Cross-linker R =	k'_D	a $(=k'_L/k'_D)$
$-O-CH_2CH_2-O-$[c]	8.4	6.4(a)
$-NH-C_6H_6-NH-$ (m)[b]	11.8	6.3(b)
$-NH-CH_2CH_2-NH-$	5.5	2.4(a)
$-NH-(CH_2)_4-NH-$	1.1	1.6(c)
$-NH-(CH_2)_6-NH-$	1.7	1.6(c)

[a] **The polymers were prepared using a monomer composition of EDMA (38 mol%), MAA (38 mol%) and the amide (or ester) cross-linker (19 mol%) in the presence of L-PheNHPh as template (4 mol%). The polymerization was carried out at 75°C under nitrogen for 48 h using AIBN (1 mol%) as initiator and MeCN as porogen (F, = 0.57). They were then crushed and washed in MeCN–HOAc (3:1) for two days whereby 30–60% of the template was recovered [as determined by HPLC (RP-18)]. The polymers were then sieved to 25-38 μm and packed into columns. In the chromatographic evaluation the retention of the D enantiomer was determined using as mobile phase: MeCN–H$_2$O–HOAc (97.5:1.25:1.25 %, v/v). Since the separation factor does not vary with the mobile phase composition the separation factors were determined at a mobile phase composition where the L enantiomer was eluted within a reasonable time. This corresponded to a composition of MeCN–H$_2$O–HOAc of (a) 95:2.5:2.5, (b) 92.5:2.5:5 and (c) 97.5:1.25:1.25 %, v/v.**
[b] **Prepared using EDMA (34 mol%) and cross-linker (23 mol%).**
[c] **Prepared using EDMA (57 mol%).**

evaluation was then performed as indicated (Table X). The amide monomers containing an aliphatic spacer gave reduced retention and selectivity compared to the ester monomers **(EDMA)**. When increasing the length of the spacer the separation factor and retention decreased. However upon introduction of an aromatic spacer, stronger binding was observed, while the selectivity was in the same order as that observed using the standard EDMA-based polymer. Since selectivity remained unchanged it is likely that the increase in binding is due to a stabilizing interaction in the site affecting both enantiomers equally [38].

CONCLUSIONS

A complete characterization of a series of photo and thermally initiated polymers imprinted with **L-PheNHPh** was performed. The materials varied widely in dry state morphology from gel-like non-porous to macroporous. The swollen state morphology however appears to be more homogeneous since a certain mass of polymer swelled to the same volume in **acetonitrile**. The largest influence on the selectivity and strength of the substrate rebinding was due to the polymerization temperature and the hydrogen bonding capacity of the porogen while the polymer morphology appeared to be less important. Photochemically initiated polymerization at low temperature and the use of a porogen with poor hydrogen bonding capacity promoted high selectivity and strong binding.

The polymers showed a high thermostability with only small variations between the polymers as judged from thermal analysis but larger variations as judged from the effect of heat treatment upon chromatographic performance (change in α, R_s and *h)*. This appeared to be related to the polymer dry state morphology where the gel-like polymers were more stable than the corresponding porous polymers (polymers prepared using different porogens). Polymers subjected to heat-treatment after polymerization showed a higher column efficiency and saturation capacity compared to the untreated polymers. This resulted in a performance comparable to some of

today's commercially available **chiral** stationary phases.

The selective rebinding of the substrate to the polymer could be inhibited by either **esterifica**-tion of the carboxylic acid groups of the polymer or by subjecting the polymers to aqueous base treatment. Finally, amide-based cross-linkers were evaluated as a possible way of introducing additional sites of interaction for the substrate. Only the aromatic-based cross-linker gave comparable selectivity to the **EDMA** polymers. This also resulted in a stronger substrate binding suggesting an additional interaction at the sites.

The data as a whole support the suggested recognition model that invoke electrostatic and hydrogen bonding interactions between the polymer and the substrate. Finally and perhaps more importantly, a porous polymer structure is not a requirement in order to achieve an efficient chromatographic matrix in molecular imprinting. Similar separations were thus seen using a non-porous swellable material and a porous material of lower swellability. This result may be informative about the domains in the polymer structure in which the recognition sites are located.

REFERENCES

1 G. Wulff, in W.T. Ford (Editor), Polymeric *Reagents and Catalysts (ACS Symposium Series, No. 308),* American Chemical Society, Washington, DC, 1986, pp. 186-230.
2 F.H. Dickey, *Proc. Natl. Acad. Sci., 35 (1949) 227.*
3 R. Curti and U. Colombo, *J. Am. Chem. Soc.,* 74 (1952) 3961.
4 G. Wulff, W. Vesper, R. Grobe-Einsler and A. Sarhan, *Makromol. Chem., 178* (1977) *2799.*
5 K.J. Shea and E.A. Thompson, *J. Org.* Chem., 43 (1978) 4253.
6 J. Damen and D.C. Neckers, *Tetrahedron Lett., (1980) 1913.*
7 L. Andersson, B. Sellergren and K. Mosbach, *Tetrahedron Lett.,* 25 (1984) 5211.
8 B. Sellergren, B. Ekberg and K. Mosbach, *J. Chromatogr., 347 (1985)* 1.
9 B. Sellergren, in R. Epton (Editor), *Innovations and Perspectives in Solid Phase Synthesis. Peptides, Polypeptides and Oligonucleotides. Macroorganic Reagents and Catalysts,* SPCC (UK), Birmingham, 1990, pp. 293-307.
10 B. Sellergren, M. Lepistö and K. Mosbach, *J. Am. Chem. Soc.,* 110 (1988) 5853.
11 B. Sellergren, *Chirality,* 1 (1989) 63.
12 L.I. Andersson and K. Mosbach, *J. Chromatogr., 516* (1990) 313.
13 M. Lepistö and B. Sellergren, *J. Org. Chem.,* 54 (1989) 6010.
14 B. Sellergren and K.J. Shea, in preparation.
15 K.J. Shea and D.Y. Sasaki, *J. Am. Chem. Soc.,* 111 (1989) 3442.
16 G. Wulff and H.-G. Poll, *Macromol. Chem., 188 (1987) 741.*
17 K.J. Shea and T.K. Dougherty, *J. Am. Chem. Soc.,* 108 (1986) 1091.
18 G. Wulff, B. Heide and G. Helfmeier, *J. Am.* Chem. *Soc.,* 108 (1986) 1089.
19 0. Norrlöw, M.-O. Månsson and K. Mosbach, *J. Chromatogr., 3% (1987) 374.*
20 D.J. O'Shannessy, B. Ekberg and K. Mosbach, *Anal. Biochem., 177 (1989)* 144.
21 B. Sellergren, *Macromol. Chem.,* 190 (1989) 2703.
22 K.J. Shea, G.J. Stoddard, D.M. Shavelle, F. Wakui and R.M. Choate, *Macromolecules, 23* (1990) 4497.
23 T. Hjertberg, T. Hargitai and P. Reinholdsson, Macromolecules, 23 (1990) 3080.
24 S.J. Gregg and K.S.W. Sing, *Adsorption, Surface Area and Porosity,* Academic Press, London, 2nd ed., 1982.
25 G. Wulff, H.-G. Poll and M. Minarik, *J. Liq. Chromatogr.,* 9 (1986) 385.
26 G.S. Weber and P.W. Carr, in P.R. Brown and R.A. Hartwick (Editors), *High Performance Liquid Chromatography,* Wiley, New York, 1989.
27 P. Reinholdsson, T. Hargitai, B. Törnell and R. Isaksson, *Angew. Macromol. Chem.*
28 Y. Kikihira and H. Yamamura, *Macromol.* Chem., 186 (1985) 423.
29 Micromeritics Corp., personal communication.
30 J. Brandrup and E.H. Immergut, *Polymer Handbook,* Wiley, New York, 3rd ed., 1989, p. VII 519.
31 J.R. Millar, D.G. Smith, W.E. Marr and T.R.E. Kressman, *J. Chem. Soc., (1963) 218.*
32 A. Guyot, in D.C. Sherrington and P. Hodge (Editors), *Synthesis and Separations Using Functional Polymers,* Wiley-Interscience, New York, 1988; Ch. 1.
33 M. Jelinkova, L.K. Shataeva, G.A. Tischenko and F. Svec, *React. Polym.,* 11 (1989) 253-260.
34 S. Jacobson, S. Golshan-Shirazi and G. Guiochon, *J. Am. Chem. Soc., 112 (1990) 6492.*
35 M. Kempe and K. Mosbach, *Anal. Lett., 24* (1991) 1137.
36 F.H. Dickey, *J. Phys.* Chem., 59 (1955) 695.
37 G. Wulff, R. Grobe-Einsler and A. Sarhan, *Macromol.* Chem., 178 (1977) 2817.
38 W.H. Pirkle and C.J. Welch, *J. Chromatogr., 589 (1992) 45.*